Vortex dynamics in classical underdamped junction arrays

H. Eikmans and J. E. van Himbergen
Institute for Theoretical Physics, University of Utrecht, P.O. Box 80 006, 3508 TA Utrecht, The Netherlands
(Received 27 September 1991)

We study the response of an array of underdamped classical Josephson junctions when the phase configuration contains precisely one vortex. We first simulate the linear response of arrays to a small oscillating current and find, as a function of frequency, a well-defined resonance apart from the single-junction resonance. When a dc current is applied, in addition to the small ac current, the resonance is seen to split into two separate peaks. Next, we analyze the full set of evolution equations and show that the response of the array under these conditions is represented very well by a set of three linear equations. With zero dc current we obtain an analytical estimate of the resonance frequency. The reduced set also reflects, but underestimates, the splitting into two resonances, in an additional dc current. Finally, we extend the approach to nonlinear response to extract one differential equation for the motion of the vortex out of the complete set of equations describing the dynamics of the array.

The interest in the dynamical properties of vortices in superconducting systems is rapidly increasing,[1–9] partly due to fact that it may be of great importance in studying the granular superconductors. Arrays of superconducting islands, weakly coupled by Josephson junctions, are very much suited to study the dynamics of these vortices because of the controlled fabrication and flexibility in varying the system parameters. Recent experimental findings in the Josephson-junction arrays[9] suggest that it is possible to reach a regime of parameters where vortex motion is ballistic. This opens up an interesting aspect in the field of transport phenomena, especially when one would be able to expose unambiguously a quantum nature of such objects, possibly in arrays of ultrasmall junctions. In understanding the results of experiments it is always crucial to have detailed knowledge of the physical properties of these objects, as for example, their mass. Therefore we perform a linear response analysis of the vortex properties in classical underdamped junctions, based on the full set of coupled evolution equations for junction arrays. Starting from this set, we first simulate the response of arrays of underdamped junctions at zero temperature, where the current distribution contains *one* vortex. The results of the response as a function of frequency, show, besides the bulk contribution, a very distinct and well-defined resonance generated by the vortex. The position of the peak in the in-phase response is the basic quantity to characterize inertial properties in the static regime. There is no strong size dependence in this position for linear system sizes larger than approximately 8, and the relative height of the peak simply decreases linearly on enlarging the system size. We also study the response as a function of an applied dc current. The resonance then splits into two peaks, reflecting the removal of a symmetry between core junctions.

Out of the complete set of equations, we then derive an effective set of only three coupled differential equations, to describe the dynamics of junction arrays in this regime. To do this we take one effective coupling parameter for all junctions *not* adjacent to the vortex core. We show, by direct comparison with the simulations, that the equations thus obtained represent the full set very well. This stresses the crucial role of the core junctions for the dynamics. In the case of an infinite system with zero dc current we reduce the set to two equations, and we express the resonance frequency in terms of the lattice Green function. In the presence of a small dc current, the reduced set exhibits the splitting of the resonance, observed in simulations, but in a less pronounced way.

Finally, we extend this approach to nonlinear behavior of a junction array with one vortex. We study the full set of equations in a model, introduced in Ref. 3, where only one junction has a sinusoidal phase-current relation. This junction is embedded in a linear medium. By taking the nonlinear junction along with the motion of the vortex, we obtain an approximate description of the response of an array with one vortex. We compare the results directly with simulations of the full set of equations, and find that the properties of the vortex itself are described quite well. However, to obtain a consistent model, one is forced to an unrealistic value for the coupling of the linear medium.

I. LINEAR RESPONSE

We consider a rectangular lattice with superconducting islands at the nodes. Each island is connected with nearest neighbors by Josephson junctions. The dynamics of single junctions is determined by the resistively shunted junction (RSJ) model, and thus the time evolution of the phase difference $\theta(\mathbf{r},\mathbf{r}',t)$ across the junction connecting islands centered at $\mathbf{r}$ and $\mathbf{r}'$ is governed by the dimensionless equation

$$\beta_c\ddot{\theta}(\mathbf{r},\mathbf{r}',t)+\dot{\theta}(\mathbf{r},\mathbf{r}',t)+i_S(\mathbf{r},\mathbf{r}',t)$$

$$+i_F(\mathbf{r},\mathbf{r}',t)=i(\mathbf{r},\mathbf{r}',t), \quad (1.1)$$

where we measure time in units of the reciprocal characteristic frequency $1/\omega_c = \hbar/(2eI_cR_n)$. $i(\mathbf{r},\mathbf{r}',t) = I(\mathbf{r},\mathbf{r}',t)/I_c$ is the total current flowing through the junction. The superconducting component $i_S(\mathbf{r},\mathbf{r}',t)$ is given by

$$i_S(\mathbf{r},\mathbf{r}',t)=\sin[\theta(\mathbf{r},\mathbf{r}',t)-2\pi A(\mathbf{r},\mathbf{r}')]. \quad (1.2)$$

The magnetic field appears in the variables

$$A(\mathbf{r},\mathbf{r}')=\frac{1}{\phi_0}\int_{\mathbf{r}}^{\mathbf{r}'}\mathbf{A}\cdot d\boldsymbol{\ell}. \quad (1.3)$$

The vector potential is $\mathbf{A}$ and $\phi_0 = hc/2e$ is the elementary flux quantum. The first term in Eq. (1.1) represents the displacement current carried by the capacitance C of the junction. The Stewart-McCumber parameter β_c is defined as

$$\beta_c=\left(\frac{\omega_c}{\omega_p}\right)^2, \quad (1.4)$$

with plasma frequency

$$\omega_p=\sqrt{2eI_c/\hbar C}. \quad (1.5)$$

The second term is the tunneling current carried by quasiparticles. In the RSJ model these processes are taken into account by shunting the junction with an ohmic resistance R_n. Apart from the intrinsic dissipative tunneling, R_n can also include an external shunt resistance. If one wants to simulate finite temperatures then one must add a noise term to the left-hand side of Eq. (1.1). However, we assume zero temperature throughout this paper.

We now briefly discuss some important properties of vortices. Physically a vortex can be seen as an eddy current in the flow pattern in a Josephson-junction array. One can assign a positive or negative charge to the vortex, depending on whether the current flows clockwise or counterclockwise. For numerical and analytical purposes it is necessary to have a rule which, given a phase configuration, determines the vorticity, or vortex charge, $M(\mathbf{R})$ at the center $\mathbf{R}$ of each unit cell. We define the value of this vortex charge to be the rotation of the gauge invariant phase differences $\varphi(\mathbf{r},\mathbf{r}')$:

$$\begin{aligned}M(\mathbf{R})&=\frac{1}{2\pi}\sum_{\text{cell}}\varphi(\mathbf{r},\mathbf{r}')\\&=\frac{1}{2\pi}\sum_{\text{cell}}[\theta(\mathbf{r},\mathbf{r}')-2\pi A(\mathbf{r},\mathbf{r}')]\\&=\Omega(\mathbf{R})-f, \quad (1.6)\end{aligned}$$

with integer $\Omega(\mathbf{R})$. Here, $\varphi(\mathbf{r},\mathbf{r}')$ is taken between $-\pi$ and $+\pi$. The sum in Eq. (1.6) is a directed sum over the bonds surrounding $\mathbf{R}$. The lattice of cell centers $\mathbf{R}$ is called the dual lattice and for each $\mathbf{r}$ we take the associated dual lattice site to be $\mathbf{R}=\mathbf{r}+(\hat{\mathbf{x}}+\hat{\mathbf{y}})/2$, with unit vectors $\hat{\mathbf{x}}$ and $\hat{\mathbf{y}}$. The parameter f measures the flux piercing a cell, in units of ϕ_0. By symmetry f can be restricted to the interval $(0,1/2)$ without loss of generality.

We write the gauge invariant phase difference over bond $<\mathbf{r},\mathbf{r}'>$ as

$$\varphi(\mathbf{r},\mathbf{r}',t)=\varphi_0(\mathbf{r},\mathbf{r}')+\delta\varphi(\mathbf{r},\mathbf{r}',t). \quad (1.7)$$

The $\varphi_0(\mathbf{r},\mathbf{r}')$ represent the reference configuration, and this is taken to be the lowest-energy state containing one vortex in the middle row. In other words, the φ_0 form the ground state of the system, under the constraint that the vortex charge as defined in Eq. (1.6) is $-f$ in all unit cells, except for one cell in the middle row, where the charge is $1-f$. These phase differences contain the magnetic field parameters $A(\mathbf{r},\mathbf{r}')$. For the boundary conditions we use periodic boundaries in the [10] direction and free boundaries in the [01] direction, together with a current bias. We also considered arrays with periodic boundaries in both directions, but these are not suitable if we want to study a configuration containing *one* vortex. Using the results of the analysis in an earlier paper,[10] we now write the set of equations for the dynamics of a junction array, in a form that enables the reduction later on:

$$\beta_c\ddot{\Phi}(t)+\dot{\Phi}(t)+<i_S(\mathbf{r},\mathbf{r}+\hat{\mathbf{y}},t)>=i_{\text{av}}(t), \quad (1.8a)$$

$$\beta_c\delta\ddot{\varphi}(\mathbf{r},\mathbf{r}',t)+\delta\dot{\varphi}(\mathbf{r},\mathbf{r}',t)+i_S(\mathbf{r},\mathbf{r}',t)$$

$$=i_{\text{av}}(t)+\sum_{\mathbf{R}'}\Delta_\perp G^s(\mathbf{R},\mathbf{R}')C(\mathbf{R}',t). \quad (1.8b)$$

Here, G^s is the lattice Green function for the lattice with the aforementioned boundary conditions. C is the circular sum of the supercurrent around the cell centered at dual lattice site $\mathbf{R}$:

$$C(\mathbf{R},t)=\sum_{\text{cell}}i_S(\mathbf{r},\mathbf{r}',t), \quad (1.9)$$

with summation in counterclockwise direction. $<i_S>$ is the spatially averaged supercurrent in the y direction, i_{av} the average current, and Φ the average phase difference. There is an equation similar to Eq. (1.8a) for bonds in the x direction. However, we only consider highly symmetrical configurations with an applied current in the y direction. Therefore, the average voltage in the x direction can be set to zero. For the present purpose it is convenient *not* to separate out the average from the variables $\delta\varphi(\mathbf{r},\mathbf{r}',t)$ directly. Consequently, Eq. (1.8a) is already included in Eq. (1.8b), but we still write it separately because this is one of the equations that will survive the reduction scheme. For other purposes it may be useful to subtract Eq. (1.8a) from Eq. (1.8b). In that case the choice of bias only appears explicitly in Eq. (1.8a). The perpendicular-difference operator in Eq. (1.8b) is

$$\Delta_\perp=\begin{cases}-\Delta_x & \text{for bonds } <\mathbf{r},\mathbf{r}+\hat{\mathbf{y}}>,\\ \Delta_y & \text{for bonds } <\mathbf{r},\mathbf{r}+\hat{\mathbf{x}}>,\end{cases} \quad (1.10)$$

where, e.g., $\Delta_x f(\mathbf{R})=f(\mathbf{R})-f(\mathbf{R}-\hat{\mathbf{x}})$.

We study linear response, and take the external current to be

$$i_{\rm av}(t) = i_{\rm ext}(t) = i_{\rm dc} + i_{\rm ac}\sin(\omega t), \text{with } i_{\rm ac} \ll 1. \quad (1.11)$$

First we set $i_{\rm dc} = 0$. The parameter β_c is set to 100, so that the individual junctions are strongly underdamped. The small quantities are Φ and the $\delta\varphi(\mathbf{r},\mathbf{r}',t)$.

Using the representation of Eqs. (1.8a) and (1.8b) we simulate the dynamics of the array. Our results are obtained in a square lattice with a linear size $L =$ 8 and 16 unit cells, and the amplitude of the oscillation is $i_{\rm ac} = 2 \times 10^{-3}$. We write the response as $\Phi(t) = A(\omega)\sin(\omega t) + B(\omega)\cos(\omega t)$ and determine the frequency dependence of A and B. In Fig. 1 we plot A and B for an 8×8 lattice with one vortex.

There is an applied magnetic field of $f = 0.025$, which corresponds to a minimum in the energy as a function of the field, given that the configuration contains a vortex. The large resonance corresponds to the bulk single-junction response. From the single-junction equation (1.1) one easily finds that the peak is located exactly at the plasma frequency, which is $\omega_p = 1/\sqrt{\beta_c}$, when time is measured in units of $1/\omega_c$. The effect of the vortex is clearly visible as a small resonance at a frequency smaller than ω_p. Because the location of this resonance is very well defined it is very useful in determining the vortex properties. In the following we concentrate on $A(\omega)$ for convenience. In fact, from the Kramers-Kronig relations we know that B does not contain any new information, once the full frequency dependence of A is known.

As we focus on the vortex part we plot A in Fig. 2 for $L = 8$ and $L = 16$. For $L = 8$ we show two graphs, one of which is taken at $f = 0.025$ and one at $f = 0$. For $L = 16$ we applied a field of $f = 0.006$ to minimize the energy. There is a significant shift between the $L = 8$ curves. Below we will explain the origin of this shift, when we discuss the reduced set of equations. There, we show that the $f = 0.025$ curve is the more appropriate, when we seek information on the properties of vortices in large systems. Comparing the $L = 16$ curve, we see that the effect of the vortex becomes smaller. Besides that, the resonance has moved to a slightly higher frequency. Assuming this to be best representation for the infinite system, our numerical result for the resonance frequency is

$$\frac{\omega_0}{\omega_p} = 0.573 \pm 0.001. \quad (1.12)$$

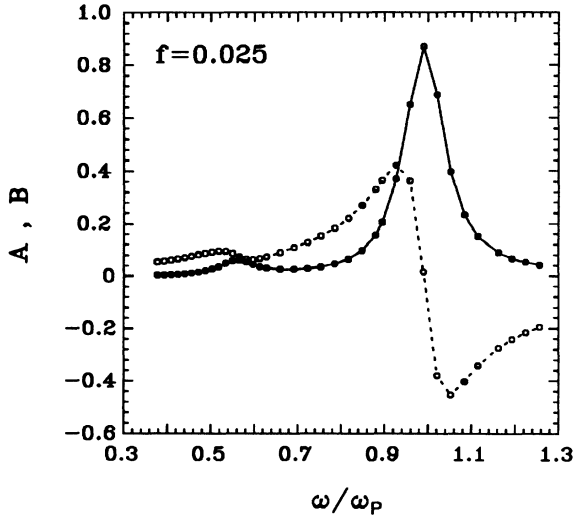

FIG. 1. Results, obtained from simulations of the full set of evolution equations, for the in-phase (solid curve) and out-of-phase (dotted curve) component of the response of an array to a current $i = i_{\rm ac}\sin(\omega t)$ with $i_{\rm ac} = 2 \times 10^{-3}$ in an 8×8 array. The curves correspond to a phase configuration with *one* vortex in the middle row.

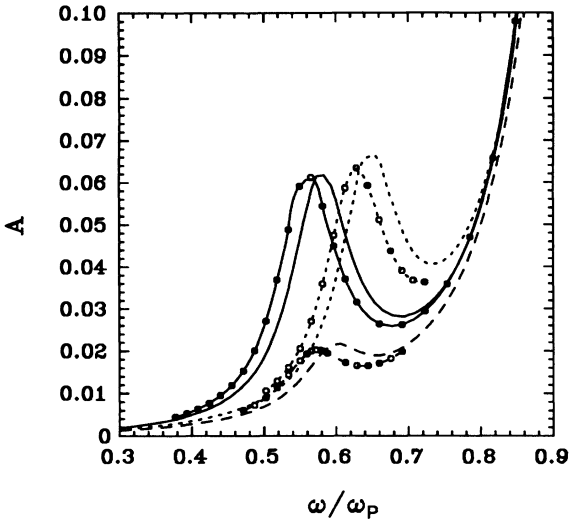

FIG. 2. The in-phase component of the response of arrays, with a phase configuration containing one vortex in the middle row. For $L = 8$ we plot a curve for $f = 0.025$ (solid curve) and for $f = 0$ (dotted curve), and for $L = 16$ we have $f = 0.006$ (dashed curve). Curves with data points are obtained from simulations, without are analytical results.

II. A REDUCED SET FOR THE LINEAR DYNAMICS

We now attempt to describe the observed features in the response by reducing Eqs. (1.8a) and (1.8b) to their essentials. First we linearize the equations around the configuration, $\varphi_0(\mathbf{r},\mathbf{r}')$, and the dual lattice position of the vortex is written as $\mathbf{R}_0$. From the extensive study of Refs. 2 and 3, as well as from continuum superconductors, we expect the vortex contribution to the response to come mainly from the core. The exceptional role of the core junctions is brought out by setting

$$\cos\varphi_0(\mathbf{r},\mathbf{r}') = \begin{cases} d_l & \text{for left-hand core junction,} \\ d_r & \text{for right-hand core junction,} \\ d_t & \text{for top and bottom core junctions,} \\ \alpha & \text{for all other junctions.} \end{cases} \quad (2.1)$$

Here, α is given by the average of $\cos\varphi_0(\mathbf{r},\mathbf{r}')$ over all junctions, except for the core junctions. We denote the gauge-invariant phase difference over the junction to the left and right of the core, by $\delta\varphi_l$ and $\delta\varphi_r$, respectively.

Substituting this in Eq. (1.8a) we obtain

$$\beta_c\ddot{\Phi}(t)+\dot{\Phi}(t)+\alpha\Phi(t)+\frac{d_l-\alpha}{N}\delta\varphi_l(t)$$

$$+\frac{d_r-\alpha}{N}\delta\varphi_r(t)=i'(t), \quad (2.2)$$

where $i'=i_{\rm ext}-<\sin\varphi_0(\mathbf{r},\mathbf{r}+\hat{\mathbf{y}})>$, which is equal to $i_{\rm ext}$ only if $i_{\rm dc}=0$. N is the number of junctions in the array. The next step is to write down similar equations for the $\delta\varphi_i$ $(i=l,r)$. By symmetry we can take the voltages over the top and bottom junctions, $<\mathbf{R_0}+\frac{1}{2}\hat{\mathbf{x}}+\frac{1}{2}\hat{\mathbf{y}},\mathbf{R_0}-\frac{1}{2}\hat{\mathbf{x}}+\frac{1}{2}\hat{\mathbf{y}}>$ and $<\mathbf{R_0}+\frac{1}{2}\hat{\mathbf{x}}-\frac{1}{2}\hat{\mathbf{y}},\mathbf{R_0}-\frac{1}{2}\hat{\mathbf{x}}-\frac{1}{2}\hat{\mathbf{y}}>$, to be identical. Consequently the corresponding phase changes can simply be expressed in $\delta\varphi_l$ and $\delta\varphi_r$. For completeness we write down the nonzero circular currents:

$$C(\mathbf{R}_0,t)=(d_r-d_t)\delta\varphi_r(t)-(d_l-d_t)\delta\varphi_l(t), \quad (2.3a)$$

$$C(\mathbf{R}_0+\hat{\mathbf{x}},t)=-(d_r-\alpha)\delta\varphi_r(t), \quad (2.3b)$$

$$C(\mathbf{R}_0-\hat{\mathbf{x}},t)=+(d_l-\alpha)\delta\varphi_l(t), \quad (2.3c)$$

$$C(\mathbf{R}_0+\hat{\mathbf{y}},t)=\tfrac{1}{2}(d_t-\alpha)[\delta\varphi_r(t)-\delta\varphi_l(t)], \quad (2.3d)$$

$$C(\mathbf{R}_0-\hat{\mathbf{y}},t)=\tfrac{1}{2}(d_t-\alpha)[\delta\varphi_r(t)-\delta\varphi_l(t)]. \quad (2.3e)$$

Inserting Eqs. (2.3a)–(2.3e) in Eq. (1.8b) we find, after some manipulations

$$\beta_c\delta\ddot{\varphi}_i(t)+\delta\dot{\varphi}_i(t)-i'(t)=A_{ii}\delta\varphi_i(t)+A_{i\underline{i}}\delta\varphi_{\underline{i}}(t), \quad (2.4)$$

with $i=l,r$, and we have defined $\underline{l}=r$ and $\underline{r}=l$. The matrix elements are

$$A_{ll}=-\tfrac{1}{2}(d_l+\alpha)+\gamma(d_t-\alpha), \quad (2.5a)$$

$$A_{lr}=-(2\gamma+\tfrac{1}{2})(d_r-\alpha)-\gamma(d_t-\alpha), \quad (2.5b)$$

$$A_{rl}=-(2\gamma+\tfrac{1}{2})(d_l-\alpha)-\gamma(d_t-\alpha), \quad (2.5c)$$

$$A_{rr}=-\tfrac{1}{2}(d_r+\alpha)+\gamma(d_t-\alpha), \quad (2.5d)$$

where we have set $\gamma=\nabla_x G^s(\hat{\mathbf{x}},0)$ and have used that

$$G^s(0,0)-G^s(\hat{\mathbf{x}},0)\approx G^s(0,0)-G^s(\hat{\mathbf{y}},0)$$
$$\approx\tfrac{1}{4}, \quad (2.6a)$$

$$\sum_{\boldsymbol{\delta}}(G^s(\mathbf{R},\mathbf{R}')-G^s(\mathbf{R}+\boldsymbol{\delta},\mathbf{R}'))=\delta_{\mathbf{R},\mathbf{R}'}, \quad (2.6b)$$

and

$$\nabla_x G^s(\hat{\mathbf{x}},0)=\tfrac{1}{2}[G^s(2\hat{\mathbf{x}},0)-G^s(0,0)]$$
$$\approx\nabla_y G^s(\hat{\mathbf{y}},0). \quad (2.6c)$$

Nearest neighbors are indicated by $\boldsymbol{\delta}=\pm\hat{\mathbf{x}},\pm\hat{\mathbf{y}}$, and 0 indicates the origin. The approximations in Eqs. (2.6a) and (2.6c) become exact in an infinite, or periodic system. With the present boundary conditions the deviation is less than 2% for an $L=8$ lattice. For large systems, the derivative in Eq. (2.6c) is approximately -0.182. (Note that the Δ and ∇ operator are not the same.) Equations (2.2) and (2.4) contain the terms in Eqs. (1.8a) and (1.8b), that are first order in the small quantities Φ and $\delta\varphi$. Because supercurrents are conserved in the configuration $\{\varphi_0(\mathbf{r},\mathbf{r}')\}$, the zeroth-order terms cancel.

We can now show that these equations do reflect the physics of our data. In Fig. 2 we plotted the analytical result, where the parameters α and d_i, extracted from the corresponding simulations, are listed in Table I. The comparison is very good, especially when we consider the enormous reduction we made of the set of equations. The peak height is practically recovered, and there is only a small, constant overestimate of the resonance frequency. Note in particular, that the shift of the $L=8$ curve with an applied field, is indeed present in the "core model," indicating that it originates primarily from a difference in the core junctions. For $f=0.025$ the current carried by the core junctions is closer to the critical current I_c (see Table I), which corresponds to an infinite array. Our results show that as a consequence of such a field, finite-size effects are diminished. For very small, e.g., $L=4$, lattices it is even essential to apply an appropriate field, because the configuration with one vortex is not stable in zero field. The analytic model shows the same decrease in peak height, if we go from $L=8$ to $L=16$, as the simulations. Also the small shift is reproduced, and in the core model it results from the slight change in α and the d_i. For an infinite system $\alpha=1$ and the d_i are zero, therefore we can conclude that the point of saturation is almost reached for $L=16$, and that our value for ω_0/ω_p is representative of infinite systems.

We now briefly consider the core model for the infinite system in zero field. Because $\alpha=1$ and $d_i=0$ $(i=l,r,t,b)$, Eqs. (2.4) can be diagonalized by introducing new variables $s=\varphi_r+\varphi_l$ and $v=\varphi_r-\varphi_l$. The equation for v does not contain the external current, therefore v is expected to be small. Furthermore, v does not appear in

TABLE I. Values of the parameters used in the core model, as obtained from simulations. Because of symmetry $d_l=d_r$ and $d_b=d_t$. We also give the values for ω_0/ω_p, as obtained from simulations of the full set of equations.

		α	d_l	d_t	ω_0/ω_p
$L=8$	$f=0.025$	0.9772	-4.41×10^{-3}	8.29×10^{-2}	0.57 ± 0.01
$L=8$	$f=0$	0.9772	0.122	-0.122	0.63 ± 0.01
$L=16$	$f=0.006$	0.9905	-1.95×10^{-3}	2.08×10^{-2}	0.573 ± 0.001

Eq. (2.2) and consequently we ignore it. The equation for s becomes

$$\beta_c \ddot{s} + \dot{s} - 2\nabla_x G(\hat{\mathbf{x}})s = i', \tag{2.7}$$

with G the (translational invariant) Green function for the infinite system. This gives a response frequency

$$\omega_0/\omega_p = \sqrt{-2\nabla_x G^s(\hat{\mathbf{x}})} \approx 0.603, \tag{2.8}$$

in reasonable agreement with the simulation result (1.12).

We now take $i_{\rm dc}$ in Eq. (1.11) to be nonzero. In Fig. 3 we present the results of the response as a function of frequency for different values of $i_{\rm dc}$. We clearly see that the resonance splits into two peaks. This is a result of the removal of the symmetry between the core junctions. Despite the off-diagonal elements $A_{i\hat{i}}$ in Eq. (2.4), each peak can still be associated by one of the core junctions. The peak that shifts to a lower frequency corresponds to the junction that is approached by the vortex. The other junction more and more resembles the junctions in the bulk. For currents above the depinning current, $i_{\rm dep} \approx 0.10$, the vortex moves through the lattice and the equations of motion can no longer be linearized. To give an overview we plotted the resonance frequency as a function of $i_{\rm dc}$ in Fig. 4. The effect of the dc current is to give a new stationary distribution $\varphi_0(\mathbf{r}, \mathbf{r}')$. We put in the parameters, obtained numerically, and in Fig. 4 we plot the resulting analytic curve next to the simulation result. The splitting is clearly present in the results obtained for the core model, though underestimated. As the dc current gets larger, the approximations made are worse because one neighboring junction, not taken into account, becomes increasingly important.

III. EXTENSION TO NONLINEAR DYNAMICS

In this section we analyze the set of evolution equations to extract *a single equation of motion* for the vortex in the array, and at the same time find the exact coupling of this equation to the measured, average quantities.

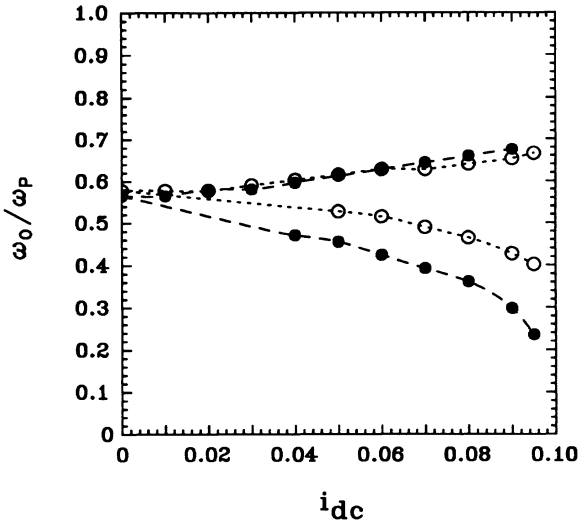

FIG. 4. Vortex resonance frequencies obtained from simulations (•), compared with analytical results (o).

First we show in Fig. 5 the current as a function of time, when the vortex configuration in the 8×8 lattice at $f = 0.025$ is exposed to a dc voltage of 10^{-4}. As a consequence the vortex moves through the lattice. We clearly see current oscillations just after the vortex has passed the energy barrier. Then the vortex slides down, and oscillates around a slowly moving "equilibrium point." We studied these oscillations for $\beta_c = 100$ and $\beta_c = 10\,000$ and found that the frequency in both cases is approximately the resonance frequency, ω_0. The frequency increases slightly in time, as the equilibrium point moves to the next junction. From this we infer that the oscillations correspond to the *high-frequency* resonance in Fig. 4. This is not unexpected because the junction

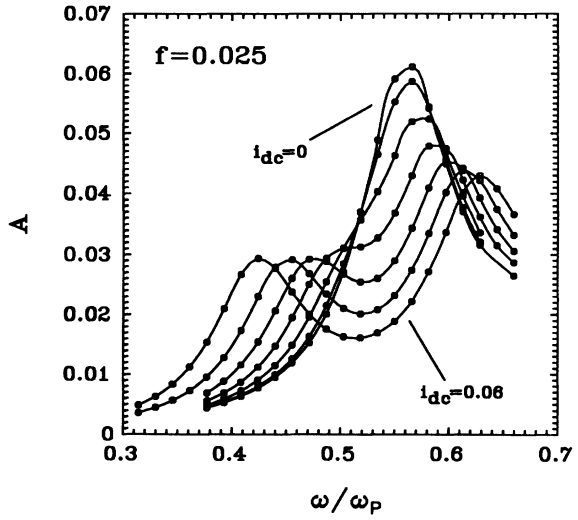

FIG. 3. The in-phase component of the response of an array to a current $i_{\rm ext} = i_{\rm dc} + i_{\rm ac}\sin(\omega t)$ with $i_{\rm ac} = 2 \times 10^{-3}$. The values of $i_{\rm dc}$ for subsequent curves differ by 0.01. The depinning current, $i_{\rm dep}$, is approximately 0.10.

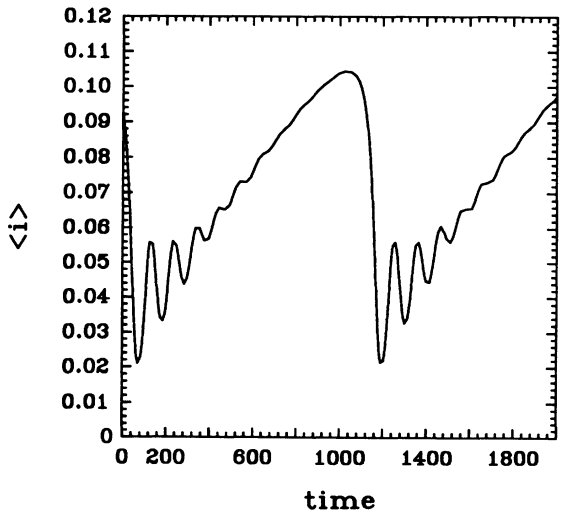

FIG. 5. Spatially averaged current as a function of time for an 8×8-array with one vortex, in a field $f = 0.025$. There is an applied dc voltage of 10^{-4}.

that is just passed by the vortex core dominates in these oscillations, and this junction is associated with the high-frequency resonance.

We now give a description, not only of the oscillations but of the full curve in Fig. 5. The model assumptions of our approach are extracted from Ref. 3. The new ingredient is, that we examine the direct consequence of this for the full set of equations, and we can directly study the consequences for the measured quantities, the average voltage or current. The model introduced in Ref. 3 consists of one nonlinear junction embedded in a linear medium. We use this "one-junction" model as a starting point to describe the nonlinear vortex characteristics, because it is the simplest possible model to contain the basic ingredients.

The coupling constant of the medium is set to α. We consider the motion of the phase difference over the nonlinear junction from $\pi/2$ to $-\pi/2$ (see Fig. 6). (In this paper we define the phase difference as drawn in Fig. 6 for the nonlinear junction.) This motion is then divided in a part where $\pi/2 \leq \varphi \leq \pi$ (I) and one where $-\pi \leq \varphi \leq -\pi/2$ (II). The restriction of φ to $(-\pi, \pi)$ is necessary to define the location of the vortex core with Eq. (1.6). The evolution equation for Φ in Eqs. (1.8a) and (1.8b) becomes

$$\begin{aligned}\beta_c\ddot{\Phi} + \dot{\Phi} &= i_{\rm av} - < i_S(\mathbf{r}, \mathbf{r}+\hat{\mathbf{y}}) > \\ &\approx i_{\rm av} - \frac{1}{N}(\sin\varphi - \alpha\varphi) - \alpha\Phi. \end{aligned} \tag{3.1}$$

We want the total current to be zero in the starting, equilibrium state, which means that $\alpha = 2/\pi$ as in Ref. 3. Because φ jumps from $+\pi$ to $-\pi$, Φ also jumps discontinuously and the net result is continuous. The equation for φ becomes

$$\begin{aligned}\beta_c\ddot{\varphi} + \dot{\varphi} &= -i_{\rm av} - \sin\varphi \\ &\quad - \nabla_{xx}G^s(0,0)[\sin\varphi - (2/\pi)\varphi] \pm 4\Delta_x G^s(0,0) \\ &\approx i_{\rm av} - \tfrac{1}{2}\sin\varphi - \varphi/\pi \pm 1. \end{aligned} \tag{3.2}$$

In Eq. (3.2), a + (−) refers to part I (II) of the motion. To obtain a quantity that varies continuously at $\varphi = \pm\pi$, we introduce

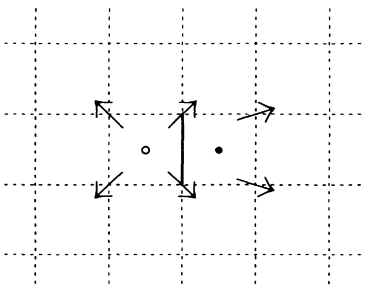

FIG. 6. One nonlinear junction (solid bar) in a linear medium (dotted bars). Initially the vortex core is at the site indicated by the open circle, and we have represented a few phases symbolically by an arrow. We analyze the set of Eqs. (1.8a) and (1.8b) for this one-junction model, and for the motion of the vortex core from the ○ to the ●.

$$x = \varphi - \mathrm{sgn}(\varphi)\pi \Longleftrightarrow \varphi = x - \mathrm{sgn}(x)\pi. \tag{3.3}$$

The equation of motion now becomes

$$\beta_c\ddot{x} + \dot{x} - \frac{1}{2}\sin x + \frac{1}{\pi}x = i_{\rm av}, \tag{3.4}$$

where x is restricted to the interval $(-\pi/2, +\pi/2)$. Note that with this definition of x, the stable equilibrium positions occur for $x = \pm\pi/2$ and not for $x = 0$. The depinning current obtained from the one-junction model is approximately 0.10 and the resonance frequency is $0.564\omega_p$, in agreement with the simulation results. In a Fourier sum the $\sin 2x$ component of $\frac{1}{2}\sin x - (1/\pi)x$ has a coefficient $1/3\pi$, which agrees with the more rigorous results of Ref. 2. Equation (3.4) is the same result as in Ref. 3. However, to obtain it we do not put in an *ad hoc* assumption or a variational form for the phase configuration. Instead we only require the vortex charge, as defined by Eq. (1.6), to have the appropriate value, which is the minimum amount of information necessary to describe the presence of a vortex. From this requirement, result (3.4) is derived by taking into account the complete set of constraints of current conservation. Besides Eq. (3.4), we obtain the precise consequences of the linear medium approximation, for the measured quantities. In fact, these measured quantities explicitly bring out the serious flaw of the one-junction model. To see this, we plot in Fig. 7 the average current as a function of time for an average dc voltage $V = \dot{\Phi} = 10^{-4}$, using Eqs. (3.1) and (3.4). To obtain this figure we extend the potential periodically, so that the x changes abruptly from $\pi/2$ to $-\pi/2$. In other words we take the nonlinear junction along with the motion of the vortex. The averaged quantities in Eq. (3.1) vary continuously in response to these jumps in x, because the average current is designed to be zero before and after the jump.

Although the plot is qualitatively the same as Fig. 5 there are important quantitative deviations. First, the

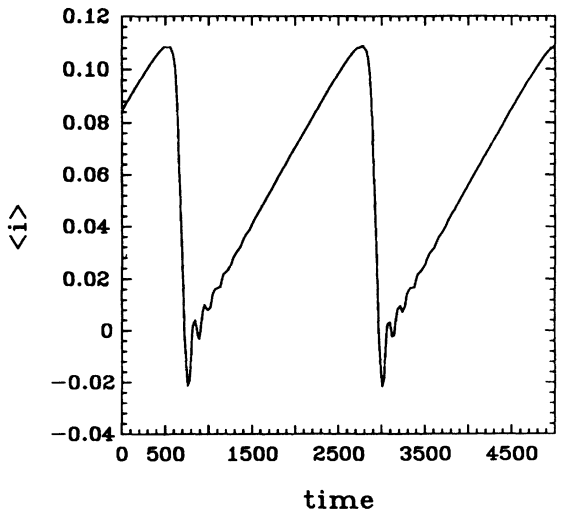

FIG. 7. Average current as a function of time for an array with a vortex, as described by the one-junction model of Eqs. (3.1) and (3.4) (see also Fig. 6).

slopes of the curves differ substantially. The values of the slopes are approximately given by the prefactors α of $\Phi(t)$ in Eqs. (2.2) and (3.1), respectively. For the real array the slope is approximately unity, as one can expect from our earlier analysis (see Table I). For the one-junction model we have taken $\alpha = 2/\pi$ to get the zero net current in equilibrium. This clearly illustrates where the model fails. In the array the current in all vortex-core junctions is ideally I_c. This means that the current of the one-core junction is compensated *by the opposite core junction*, and the rest of the medium transports little; i.e., α is close to unity. In the model we have spread this return current over all junctions, with no special role played by the opposite core junction, leading to $\alpha = 2/\pi$. With this knowledge of the major weak spot it may be possible to improve on the model. As a first attempt one can assign a separate linear coupling α' to the other core junction, in order to take into account its exceptional position. Then one has to impose the proper continuity conditions at the point where the bonds are shifted along with the motion of the vortex. In the model above, the continuity is automatically satisfied. Such an approach may allow for improvement upon the value of the slope. At this point it is hard to predict whether this also helps to resolve some other deviations, of the results of the one-junction model, from simulation results: there is a small region with a negative net current in the one-junction model, and the amplitude of the oscillations in this region is smaller than in the simulations. Therefore, further study is necessary to see if such an approach can indeed yield a set of two equations, which reflects the full set quantitatively, perhaps in a limited regime of vortex velocities.

Finally, we repeat that our results pertain to the underdamped classical regime because our approach is based on the classical Langevin equations. Experimentally, both underdamped classical junction arrays and arrays in the quantum regime are of great current interest.[8,9] Although our method is not applicable to the latter, the classical resonance frequencies of vortices described in this work are expected to be important physical parameters in the quantum regime as well.

ACKNOWLEDGMENTS

This work is part of the research program of the "Stichting voor Fundamenteel Onderzoek der Materie (FOM)," which is financially supported by the "Nederlandse organisatie voor Wetenschappelijk Onderzoek (NWO)."

[1] For a general review see, *Proceedings of the NATO Advanced Research Workshop on Coherence in Superconducting Networks, Delft, The Netherlands*, edited by J. E. Mooij and G. B. J. Schön [Physica B **152**, 1-302 (1988)].

[2] U. Eckern and A. Schmid, Phys. Rev. B **39**, 6441 (1989).

[3] A. I. Larkin, Yu. N. Ovchinnikov, and A. Schmid, in *Proceedings of the NATO Advanced Research Workshop on Coherence in Superconducting Networks, Delft, The Netherlands* (Ref. 1), p. 266.

[4] S. E. Korshunov, in *Proceedings of the NATO Advanced Research Workshop on Coherence in Superconducting Networks, Delft, The Netherlands* (Ref. 1), p. 261.

[5] B. J. van Wees, Phys. Rev. Lett. **65**, 255 (1990).

[6] T. P. Orlando and K. A. Delin, Phys. Rev. B **43**, 8717 (1991).

[7] T. P. Orlando, J. E. Mooij, and H. S. J. van der Zant, Phys. Rev. B **43**, 10 218 (1991).

[8] H. S. J. van der Zant, F. C. Fritschy, T. P. Orlando, and J. E. Mooij, Phys. Rev. Lett. **66**, 2531 (1991).

[9] H. S. J. van der Zant, F. C. Fritschy, T. P. Orlando, and J. E. Mooij (unpublished).

[10] H. Eikmans and J. E. van Himbergen, Phys. Rev. B **41**, 8927 (1990); H. Eikmans, J. E. van Himbergen, H. S. J. van der Zant, K. de Boer, and J. E. Mooij, Physica B **165&166**, 1569 (1990).